ACS OMEGA

http://pubs.acs.org/journal/acsodf

Article

First-Principles Model to Evaluate Quantitatively the Long-Life Behavior of Cellulose Acetate Polymers

Abeer Al Mohtar,* Sofia Nunes, Joana Silva, Ana Maria Ramos, João Lopes, and Moisés L. Pinto*

Cite This: *ACS Omega* 2021, 6, 8028–8037

Read Online

ACCESS | Metrics & More | Article Recommendations | Supporting Information

ABSTRACT: A deep understanding of the degradation of cellulose diacetate (CDA) polymer is crucial in finding the appropriate long-term stability solution. This work presents an investigation of the reaction mechanism of hydrolysis using electronic density functional theory calculations with the B3LYP/6-31++G** level of theory to determine the energetics of the degradation reactions. This information was coupled with the transition-state theory to establish the kinetics of degradation for both the acid-catalyzed and noncatalyzed degradation pathways. In this model, the dependence on water concentration of the polymer as a function of pH and the evaporation of acetic acid from the polymer is explicitly accounted for. For the latter, the dependence of the concentration of acetic acid inside the films with the partial pressure on the surrounding environment was measured by sorption isotherms, where Henry's law constant was measured as a function of temperature. The accuracy of this approach was validated through comparison with experimental results of CDA-accelerated aging experiments. This model provides a step forward for the estimation of CDA degradation dependence on environmental conditions. From a broader perspective, this method can be translated to establish degradation models to predict the aging of other types of polymeric materials from first-principles calculations.

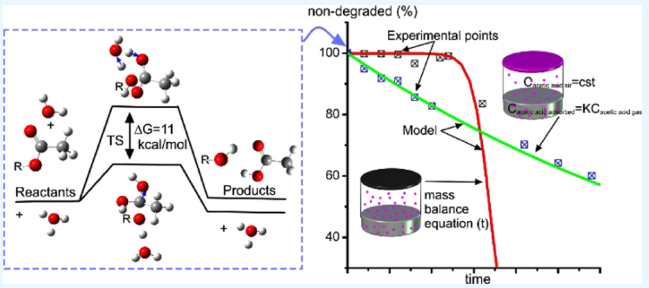

INTRODUCTION

The production of new polymeric materials at the industrial scale during the 20th century led to their widespread use for several applications ranging from biomedical[1] applications to electrical/electronic/optoelectronic applications.[2,3] The stability of these synthetic polymers is a critical issue for technological applications, for which the degradation of the polymer, also called "aging", and the performance loss over time need to be carefully evaluated.[4,5] To this aim, several methodologies have been developed and are commonly accepted to compare polymer performance.[6,7] For technological applications, the polymer stability needs to be assured for its expected useful lifetime, which is usually less than 30 years. Polymers also started being extensively used to produce artworks and several other cultural objects. A significant number of cultural heritage objects of the 20th century are made of, or contain, synthetic polymers. However, for a cultural asset, the stability needs to be assured for much longer periods than for technical applications. In this work, we present the very challenging and important case of the semisynthetic polymer cellulose acetate (CA). The use of this polymer as a film base in photography and motion-picture was first introduced by Kodak in the 1920s to substitute the flammable cellulose nitrate. Cellulose diacetate (CDA) was later substituted by the chemically and physically more stable cellulose triacetate (CTA). The use of cellulose acetate polymers was widespread in the photographic and cinematographic industry during the next few decades. These polymers now represent a significant percentage of audiovisual archives all over the world. Unfortunately, cellulose acetate-based films proved to be less permanent than expected, and this heritage is now irreversibly degrading.[8] However, the long-term stability/degradation of CA is not sufficiently understood to guarantee innovative and efficient strategies for its long-term preservation. It is important to highlight that this particular polymer is of enormous importance for our collective history. A significant part of the memoirs of the 20th century was recorded in films, photographs, and audio tapes made with CA that need to be preserved. We present in this work our contribution to this challenging problem by establishing a first-principles model that can be used to estimate the polymer's stability under variable environmental conditions. This approach may be of interest to be extended to other polymeric materials.

Some studies have been performed to understand the degradation pathways and the factors involved in the degradation of CA items.[9,10] It is now known that

Received: November 7, 2020
Accepted: February 4, 2021
Published: March 17, 2021

deacetylation under neutral and acid-catalyzed conditions are the two primary degradation mechanism. However, CA degradation depends on extrinsic factors like temperature, relative humidity (RH), and pH of the surrounding environment and on intrinsic factors related to the material composition (degree of substitution (DS) of acetyl groups, presence of other compounds—manufacturing residues, plasticizers, additives). The dependence on all of these factors and the autocatalytic degradation mechanism (presented below) make the prediction of the degradation of this polymer a difficult task. Moreover, the explicit dependence of the degradation of CA on these factors and the kinetics of the degradation mechanisms are still unknown. Some studies have performed accelerated aging experiments to predict the lifetime dependence on these parameters of historical films made of CA to provide a guide to the best storage conditions.[11,12] However, these studies did not take into account the autocatalytic behavior of the deacetylation process, which leads to an overestimation of the film's lifetime. Much data has been gathered also from accelerated and naturally aged films. The data were fitted to the Arrhenius equation to give an idea about the activation energy of the reaction(s) leading to the degradation.[13] A more recent study suggested a new model to determine the long-life behavior of CTA.[14] However, like the previous studies, this model is a data-based model, where the model is fitted to the experimental data. Moreover, all of the presented studies disregarded the volatility of acetic acid (AA), which is a crucial parameter. In other words, a quantitative understanding of the degradation mechanisms and the chemistry behind them is still missing.

In this work, we develop a first-principles model based on kinetic equations that describes the behavior of the CDA polymer, chosen because its instability is higher than that of cellulose triacetate. The aim of this study is to improve the fundamental understanding of the chemistry of degradation of this material and thus find a more appropriate and sustainable solution to extend the lifetime of the CDA polymer. The developed model includes the main degradation mechanisms, namely, deacetylation reaction under neutral conditions and acid-catalyzed deacetylation. Since the values of the kinetic constants for the deacetylation reactions of CDA are not known, we first made an attempt to calculate the activation Gibbs energy values from first-principles quantum chemical calculations using the density functional theory (DFT) formalism with clusters representative of the polymer structure. Later, the model was developed in the framework of the transition-state theory (TST) to calculate the kinetic constants of the reactions. The volatility of AA from CDA is not available in the literature, and thus we measured Henry's law constant to quantify the phase equilibria of AA between gas and CDA sorbed phases. The rate and mass balance equations were finally used to calculate the evolution of deacetylation with time. This model provides further insights into the role of AA as a reaction product and catalyst of the degradation process and how its accumulation on the polymer or the surrounding environment influences the degradation rate. Accelerated aging experiments were performed, and the pure CDA films were characterized by micro-Fourier transform infrared (μFTIR) spectroscopy to determine the degree of acetate substitution, *i.e.*, the degree of degradation. The developed model was then compared to the experimental results. In this work, the experimental data of accelerated aging was not used to fit any parameter in the model; it was rather used as a benchmark to evaluate the accuracy of the developed model and the validity of our approach.

MATERIALS AND METHODS

Computational Methods. DFT[15] calculations were performed using the Gaussian09[16] software package. Becke's three-parameter hybrid exchange functional combined with the Lee−Yang−Parr correlation functional (B3LYP)[17] was used with the 6-31++G** basis set (B3LYP/6-31++G**). This level of theory was chosen because it can accurately describe the hydrolysis of simpler systems such as methyl acetate hydrolysis.[18] The B3LYP/6-31++G** was used to optimize the structures (reactants, products, and intermediates), search for the transition states, and calculate the vibrational frequencies as well as the energies of the different structures. The right transition states were confirmed through the verification of the imaginary vibrational frequencies involving the bonds being broken and those being formed. Since the studied polymer contains a significant amount of water, two or three water molecules coordinating with oxygen atoms on one acetyl group were considered in the cluster models. This accounts for the existing hydrogen bonding as well as other intermolecular interactions of water near the reactive sites.

The rate of reactions was calculated based on the TST, which is essential for simulating long time-scale dynamics. Considering the reaction coordinate that represents the atomic displacement, $\Delta S^{\ddagger}$ and $\Delta H^{\ddagger}$ are the maximum changes in entropy and enthalpy, respectively, that correspond to the transition state. The rate is expressed as

$$k = \frac{K_B T}{h} \exp\left(\frac{\Delta S^{\ddagger}}{R}\right) \exp\left(-\frac{\Delta H^{\ddagger}}{RT}\right) \quad (1)$$

where K_B, h, and R are Boltzmann's, Plank's, and perfect gas constants, respectively, and T is the temperature. At first impression, this equation seems to describe a first-order rate constant. However, the TST is derived for bimolecular reactions. This apparent problem arises from different ways of expressing the concentration units, where they are included in the units of rate constant and omitted for equilibrium constants.[19] Upon homogenizing the units of concentration, the rate equation can be obtained

$$\frac{dC_A}{dt} = -\frac{K_B T}{h} \exp\left(\frac{\Delta S^{\ddagger}}{R}\right) \exp\left(-\frac{\Delta H^{\ddagger}}{RT}\right) \frac{C_A C_B}{C_s} \quad (2)$$

C_s is the standard concentration (usually 1 mol/L), which is a normalization term that is needed when using units of concentration other than Molar. C_A and C_B are the concentrations of reactants in a chemical reaction. In the current work, C_A is the concentration of acetyl groups in the CDA polymer. *In the deacetylation process under neutral conditions,* C_B is the concentration of water inside the polymer. In the deacetylation process under acid-catalyzed conditions, C_B is the concentration of acetic acid, responsible for the production of the H_3O^+ ion. The Wigner tunneling correction[18] had no significant effect on the rate calculations, and for this reason, it was not considered in this study.

Synthesis of Pure CDA Polymer Films. CDA films were prepared by dissolving 1 g of the polymer (cellulose acetate 39.7 wt % acetyl content, ρ = 1.3 g/cm^3, Aldrich) in 100 mL of a mixture 1:1 chloroform (high-performance liquid chromatography (HPLC) grade, Aldrich) and acetone solvent,

https://dx.doi.org/10.1021/acsomega.0c05438
ACS Omega 2021, 6, 8028−8037

respectively (p.a. Aldrich, 99.8%), inside Erlenmeyer flasks. The mixtures were maintained under stirring for 24 h. Then, the solutions were poured into individual glassware with a flat base (such as Petri dishes). The solvents were left to evaporate in a fume cupboard, and the films were considered dried, without solvent residues, upon reaching constant weight. They were kept in a desiccator until testing. The thickness of the CDA films was measured with a micrometer and was ca. 200 μm. The films were cut in 4 cm × 4 cm pieces and placed in glass supports.

Accelerated Aging. Two sets of artificial aging conditions were performed for triplicate films. The first set of experiments was thermal aging, where the CDA films were aged inside an oven at 80 °C. Goblets with distilled water were placed inside the oven to achieve about 100% RH. The second set of experiments was acidic aging, where CDA films were aged inside a desiccator placed inside an oven at 70 °C. The acetic acid solutions were prepared at a concentration of 2% (weight percentage), following the procedure proposed by Cruz et al.[20] Each week in the beginning and later at the time of collecting the sample for analysis, the desiccator was cleaned (washed) and the solution was replaced with the initial volume and concentration. Prepared solutions correspond to a molar fraction of 0.0064 in the liquid phase. To determine the molar fraction in the gas phase, or the partial pressure of acetic acid, P_{AA}, the nonrandom two-liquid model coupled with the Hayden−O'Connell equation of state (NRTL-HOC)[21] is considered using ASPEN Plus process simulation software. This method is recommended for highly nonideal chemical systems with carboxylic acids.[22,23] It reliably predicts solvation and dimerization in the vapor phase, which is particularly useful with mixtures containing carboxylic acids. This method gives, for the used experimental aqueous concentration and temperature conditions, a value of P_{AA} = 37.57 Pa. To calculate the concentration in the gas phase, we considered the gas compressibility factor Z, expressed as function of P (in Pa), as

$$Z = 0.351 + 0.729P^{-0.176} \quad (3)$$

This expression is provided by Cruz et al.[24] upon fitting data obtained by MacDougall et al.[25] Calculating the concentration of AA in the gas phase taking into consideration the gas compressibility $Z(P_{AA})$ of 0.736 gives a concentration of 1.7899×10^{-5} mmol/cm^3. This concentration is implemented in the developed model for the AA concentration in the vapor phase, in the acidic aging conditions (*i.e.*, constant acetic acid concentration in the gas phase). The AA solution was replaced each week, and the acidic aging chamber was cleaned to maintain constant conditions. A total aging of 29 weeks was performed within the framework of this study.

μ-FTIR Spectra. Infrared analysis was performed with a Nicolet Nexus spectrometer coupled to a Continuum microscope (15×) and an MCT-A detector cooled by liquid nitrogen. FTIR spectra were collected in the transmission mode from 4000 to 650 cm^{-1} on micro samples compressed with a Thermo diamond anvil cell. A total of 128 scans on each sample were performed to improve the signal-to-noise ratio while fixing the spectral resolution at 8 cm^{-1}. Spectra acquisition was performed using Omnic E.S.P. 5.2 software. The degree of substitution (DS, the number of acetyl groups by the anhydroglucose ring of the polymer repeating unit) of the samples (collected always from the same film, at three different points) was calculated from the obtained triplicated IR spectra. Following the study conducted by Fei et al.,[26] an experimental calibration curve was obtained[27]

$$y = 0.4916\mathrm{DS} + 0.1528 \quad (4)$$

with y being the ratio between the intensity of the C−O peak (at 1240 cm^{-1}) and that of the C−O−C peak (at 1050 cm^{-1}). This ether bond between the two anhydroglucose rings only suffers variation if chain scission of the polymer occurs, which is not the case considered. This method of determining the DS has been followed by several groups[28] owing to the invariant nature of the C−O−C functional group and the possibility of using it as a reference peak.

Sorption of Acetic Acid on Cellulose Acetate. To determine Henry's constant for the sorption of AA on cellulose acetate, about 50 mg of pure CDA films was placed on a microbalance (CI Electronics) under a controlled temperature of 25 °C (VMR, VWB2 series, temperature stability 0.2 °C). The samples were outgassed for about 30 min under vacuum. After purification with freeze−vacuum−thaw cycles inside a vacuum cell, AA was evaporated into the microbalance and the mass increase as a function of time was recorded. After reaching equilibrium, the pressure (MKS a-BARATRON capacitance manometer, 10 Torr-range) of AA inside the system and mass increase of the sample were considered as equilibrium points. The obtained isotherms were fitted to a linear relation (see the Supporting Information (SI) for more information).

RESULTS AND DISCUSSION

To have a deep understanding on and quantitative assessment of the long-term behavior of the CDA polymer, the TST rate equation (eq 2) has been applied. The application of this equation requires the Gibbs free energy of activation or the entropy and the enthalpy change of the reaction along with the concentration evolution of each reactant as a function of time. In this study, we concentrate on the two main degradation channels, namely, deacetylation under neutral conditions as well as acid-catalyzed deacetylation, discussed in the two following sections. The structure of the transition state for each reaction step needs to be determined so that the energy barrier of the limiting step is taken into account. Since the experimental measurement of these quantities is very difficult, we opted to estimate them using a DFT approach. The concentration profiles of each reactant, namely, that of water and the hydronium ion, need to be determined as a function of the various parameters: temperature (T), relative humidity (RH), and pH. These values can be determined experimentally. Different studies in the literature reported experimental data on the concentration of water in cellulose acetate polymers as a function of these parameters.[29−31] The provided data were fitted, and the resulting equation was used, as detailed below. However, no such data were reported for the AA concentration in the CA polymer. Knowing that the AA produced by the deacetylation reaction under neutral conditions is the precursor of the hydronium ion and the fact that it is a volatile compound, it was mandatory to measure the phase equilibrium constants (gas and adsorbed phases) to determine the concentration of AA left in the film. In the following sections, we detail the steps taken to reach the final model.

Energy Barriers for Deacetylation under Neutral Conditions. Deacetylation under neutral conditions, which is an inevitable reaction due to the presence of moisture inside

https://dx.doi.org/10.1021/acsomega.0c05438
ACS Omega 2021, 6, 8028−8037

Scheme 1. Proposed Mechanism for CDA Deacetylation under Neutral Conditions[a]

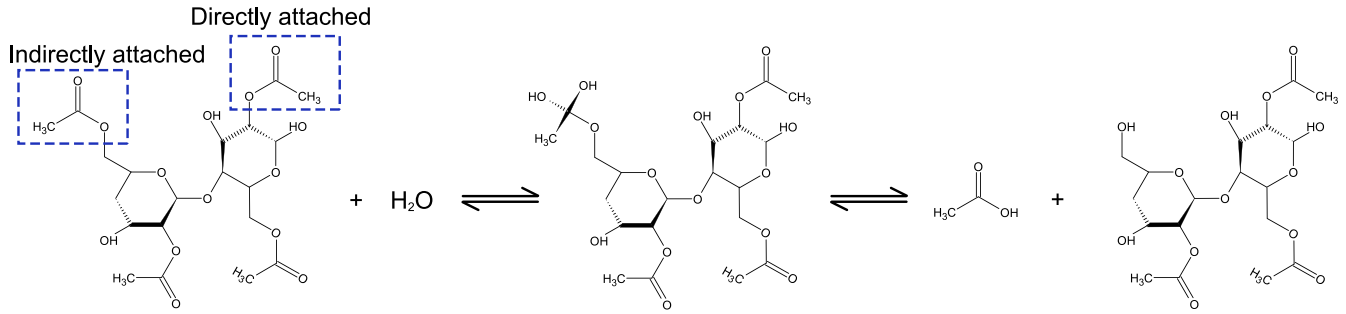

[a]Only the hydrolysis of the indirectly attached group is shown for simplicity, although both directly attached and indirectly attached acetate groups follow similar mechanisms.

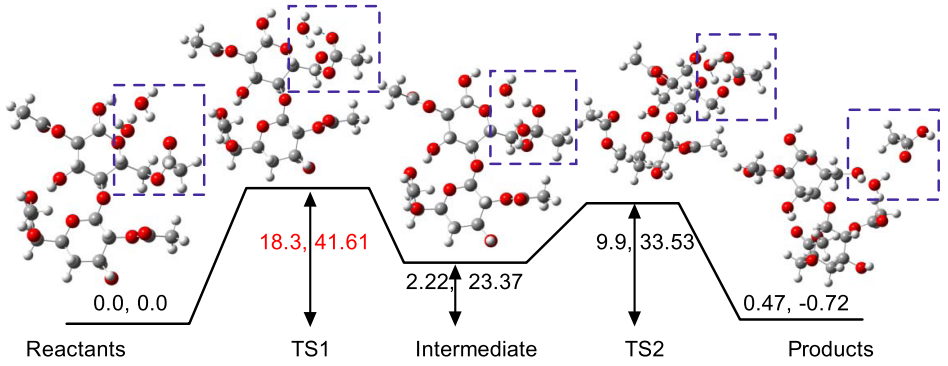

Figure 1. Enthalpies and Gibbs energies, ΔH and ΔG (kcal/mol), at 25 °C and atmospheric pressure, calculated with the DFT method, for the reactants, products, intermediates, and transition-state structures that are involved in the CDA deacetylation process under neutral conditions.

Scheme 2. Proposed Mechanism for Deacetylation of CDA under Acid-Catalyzed Conditions

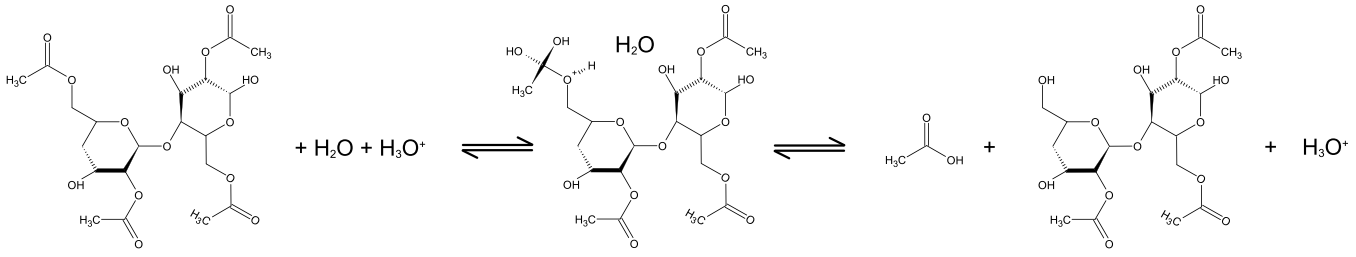

films, is the degradation channel considered in this section to calculate the energy barriers of the step reactions with the DFT method. Scheme 1 represents the sequence of the reaction and the structure of the cluster model used to represent the monomer. Two types of acetyl groups, directly and indirectly attached to the glucose ring, as highlighted in Scheme 1, were considered for the calculations. A small difference between the results was obtained for both cases and was considered within the error of the method. For clarity, the second reaction chain, *i.e.*, acid-catalyzed deacetylation, which is an autocatalytic reaction, is described and discussed in the next section.

Considering the known reactants and products, and the expected intermediate structure, a considerable computational effort was made to locate the transition states that correspond to the breaking/formation of the desired bonds. Figure 1 shows the results of the DFT calculations, where the two-step reaction with an unstable intermediate can be seen. In the reactants, two water molecules coordinating through hydrogen bonds with the oxygen atom were considered in the system although only one reacts with the carbonyl carbon. This was essential to have a concerted proton exchange that can be depicted in the transition-state 1 (TS1) structure. This finding is in agreement with previous results of Xia and Zhang,[18] where several water molecules were also considered to obtain a transition state of the methyl acetate deacetylation. The additional water molecule also plays a critical role again in the second reaction step because it helps in the concerted proton exchange from the OH group to the bridging oxygen, as can be seen in the transition-state 2 (TS2) structure (Figure 1).

As can be observed from the energy diagram in Figure 1, the first step is the limiting step for this reaction chain, where the C═O is converted into C−OH due to the addition of an extra hydrogen atom. In the same step, a deprotonated hydroxyl group is attached to the carbonyl atom of the acetyl group under dissociation. This step corresponds to a higher energy barrier than the second step of acetyl group detaching. Thus, the obtained values of 18.3 and 41.61 kcal/mol for ΔH and ΔG, respectively, are the relevant values that were implemented in the TST rate equation (eq 2). In addition to the energy barrier calculations, the bond lengths and angles

https://dx.doi.org/10.1021/acsomega.0c05438
ACS Omega 2021, 6, 8028−8037

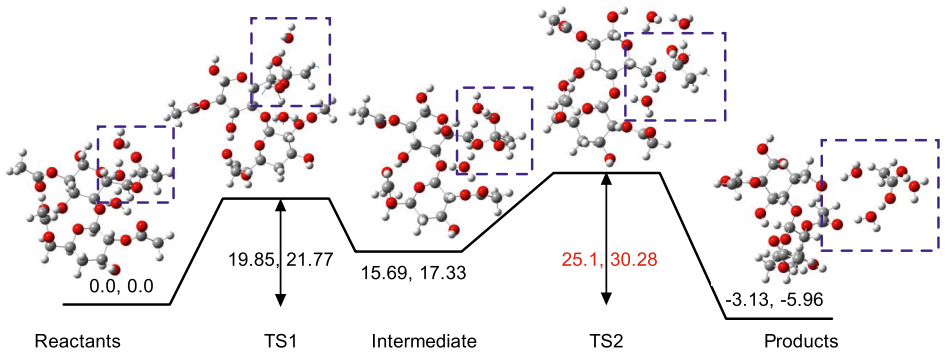

Figure 2. Enthalpies and Gibbs energies, ΔH and ΔG (kcal/mol), at 25 °C and atmospheric pressure, for CDA deacetylation under acid-catalyzed conditions, calculated at the B3LYP/6-31++G** level of theory.

Table 1. Standard Molar Enthalpy, Entropy, and Gibbs Energies of Reaction and of Activation for Deacetylation under Neutral Conditions and Acid-Catalyzed Conditions

energies (kcal/mol)	$\Delta_r H°$		$\Delta_r G°$		$T\Delta_r S°$		$\Delta_{\ddagger} H°$		$\Delta_{\ddagger} G°$		$T\Delta_{\ddagger} S°$	
state	inter.	prod.	inter.	prod.	inter.	prod.	TS1	TS2	TS1	TS2	TS1	TS2
neutral conditions	2.22	−1.75	23.37	−24.09	−21.15	22.34	18.3	7.68	41.61	10.16	−23.31	−2.48
acid-catalyzed conditions	15.69	−18.82	17.33	−23.29	−1.64	4.47	19.85	9.41	21.77	12.95	1.92	6.9

as well as the orbitals can be inferred from these calculations. In Figure 1, only the calculations performed for the deacetylation reaction of an acetyl group indirectly attached to the cellulose ring are shown. However, calculations were also performed for deacetylation of an acetate group directly attached to the cellulose ring, giving very similar results. It is also worth mentioning that the energy of the products is almost the same as that of the reactants, revealing the fact that this polymer is very stable, with respect to deacetylation under these conditions, and that no degradation is expected to occur if there is no acidification of the medium.

Energy Barriers for Deacetylation under Acid-Catalyzed Conditions. Scheme 2 is the proposed mechanism for the reaction in an acidic medium. McGath et al.[10] presented a similar mechanism; however, in this work, the steps of protonation are disregarded since these steps are very quick with low energy barriers in comparison to that of the dissociation of the C═O double bond as well as the detaching of the acetyl group.

After structure optimization of the charged reactants, products, and the intermediate, the search for the transition states was conducted, which is rather a difficult task especially in the presence of charges. The TS has one imaginary frequency involving the atoms displaced in the reaction. A video evidencing this phenomenon is provided in the Supporting Information. If the initial guess for the TS structure is not sufficiently close to the saddle point, wrong results are obtained (*i.e.*, breaking/formation of other bonds that would not lead to the desired products) or convergence difficulties arise. Moreover, to ameliorate convergence, the calculation of forces was done at the beginning of the optimization. Since in this work we are dealing with molecules with a relatively high number of atoms, the calculations are quite computationally expensive. Thus, we opted to first find a good guess for the TS at a lower level of theory (B3LYP/6-31) and, then with the obtained result, start the calculations at the required level of theory to obtain the accurate values. Figure 2 shows the results obtained for the acid-catalyzed deacetylation process. It also revealed a two-step reaction with a very unstable intermediate. Two water molecules and one hydronium ion were initially coordinating with the oxygen atom to account for the hydrogen bonds. We notice that, in this reaction, the detaching of the acetate group to form AA is the limiting step, contrary to the previous noncatalyzed case. In fact, comparing the two situations (Figures 1 and 2), the initial activation step is the one that decreases significantly when a proton is considered in the mechanism. Thus, the values of the second step of 25.1 and 30.28 kcal/mol are the values implemented in eq 1 to estimate the reaction rate. It is important to note that this degradation channel is much quicker than the first one with a reduction of 7.89 kcal/mol in the Gibbs free energy of activation. Also, note that the products in this reaction are more stable than the reactants, indicating that this reaction is favored. Table 1 reports the standard molar Gibbs energies, enthalpies, and entropies of the reaction as well as of activation. The role of AA as a catalyzer of the reaction is spotlighted through the energy barrier reduction ($\Delta_{\ddagger} G°$) of the first step (TS1) by about 20 kcal/mol. The entropic behavior, reported in Table 1, follows the described mechanism, where for the intermediate state a decreased entropy is observed since it corresponds to a combined molecular state. However, for the products, an increased entropy is noticed, emphasizing the stability of the products as well as the formation of the AA molecule.

Calculations of Concentrations in the Polymer. To calculate the rate of reaction using eq 2, the concentration of water in the polymer needs to be known, preferably as a function of the relative humidity, temperature, and pH of the polymer, including the concentration of the H_3O^+ ion inside the polymer. The methods followed and the measurements made to obtain these quantities are presented next.

All of the concentrations in the rate equation (eq 2) are expressed in mmol/g. The standard concentration, C_s, which is 1 M, becomes in our representation $C_s = 1\ \text{M}/\rho_{\text{polymer}} = 0.704$ mmol/g, with the density of CDA, $\rho_{\text{polymer}} = 1.3$ g/cm^3. The initial concentration of acetyl groups in the CDA polymer is expressed as a function of DS: C_0 = DS × 1000/(anhydroglucose molar mass + DS × acetyl group molar mass), where the anhydroglucose molar mass of the cluster is

https://dx.doi.org/10.1021/acsomega.0c05438
ACS Omega 2021, 6, 8028−8037

171.15 g/mol and the acetyl group molar mass is 59.04 g/mol. The concentration of H_2O as a function of relative humidity (RH) and temperature of the surrounding environment was fitted from the data presented by Adelstein et al.[29] In that work, they provide two different sets of data, one for the concentration of H_2O as a function of RH and the latter as a function of the temperature. These sets were fitted to one equation with two independent variables (RH, T). Although the data was given for CTA, higher moisture regain for the diacetate is expected. However, the model is not very sensitive to small variations in the initial concentration of water (±20%). The water retention as a function of pH was determined from data obtained by Allen et al.,[30] where the weight percentage of the mass increase was reported. The data were fitted, and the resulting dependence was added to eq 5 (additional information in the SI). Expressing the H_2O concentration in mmol/g as a function of these parameters, we get

$$C_{H_2O} = 2.34 + 0.027 \times RH - 0.007 \times T + 3.96 \times 10^{11} pH^{-20.29} \quad (5)$$

To calculate the rate of the acid-catalyzed reaction, the concentration of H_3O^+ should be determined, which will lead to the lowering of the pH inside the polymer. Acetic acid is the main factor responsible for the formation of the hydronium cation due to its dissociation with water

$$CH_3COOH + H_2O \rightleftharpoons CH_3COO^- + H_3O^+$$

Acetic acid is the product of the water hydrolysis reaction of CDA; thus, the maximum total amount of AA inside the polymer at time t is the total amount produced, assuming that initially no AA was present (initial boundary conditions for the differential eq 2). Taking into account the fact that AA is a volatile entity, the amount of AA that stays inside the film was estimated through Henry's law (see details in the SI).

Henry's law constant was measured for new polymer films as well as for those aged to about 10% loss in DS, and the same values were obtained. Henry's law constant was measured at room temperature (25 °C) as well as at the temperature of accelerated aging experiments (70 °C). Table 2 presents the obtained values (more information and details are presented in the SI).

Table 2. Henry's Law Constant in Different Forms

	Estimated Henry's constant	
temperature (°C)	mmol AA/g CA	cm^3/g CA
25	20.65 ± 1.48	24 215 ± 1456
70	21.72 ± 1.24	3334 ± 227

Note that while using Henry's law in the form

$$Q_{in} = K_H(p/p^0) \quad (6)$$

with Q_{in} being the concentration of AA inside the film and p and p^0 being the corresponding pressure and saturation pressure of AA (at temperature T), the K_H value is found to be almost independent of temperature for the measured temperature range (25 and 70 °C) when expressed in this form.[32] As can be seen in Figure S1b, for the investigated range of p and T, the influence of T is compensated in the relative pressure (p/p^0), and thus, the estimated Henry constant can be regarded as temperature-independent. However, for practical reasons, we are interested in expressing the concentration of AA inside the film (mmol/g) as a function of the concentration outside the film C_{out} (mmol/cm^3). Inserting in eq 6 the gas law, accounting for the nonideality of AA, $pV = nZRT$, we get

$$Q_{in} = K_H \frac{ZRT}{p^0}\left(\frac{n}{V}\right) = K'_H C_{out} \quad (7)$$

with

$$K'_H = K_H \frac{ZRT}{p^0} \quad (8)$$

the temperature-dependent Henry's law constant expressed in cm^3/g as a function of the temperature-independent Henry's law constant K_H in mmol/g and Z is the compressibility reported as a function of pressure (eq 3). Having a closer look at Z, for very low pressures, it yields values higher than 1, the ideal gas case. For this reason, implementing it directly in the model and calculating it as a function of time lead to some misleading results. This coefficient was determined by postprocessing. In other words, the partial pressure of AA was determined and then the compressibility factor was calculated at each point. It is found that this coefficient varies little, in the region of interest, where it is relevant. An average of $Z = 0.691 \pm 0.006$ is found. The mass balance equation (eq 9) was used to determine the concentration of AA inside the film at time t. Q_{in}, can be calculated as a function of the concentration produced (eq 10), where Q_0 is calculated considering no release of AA (*i.e.*, total amount of AA produced from $t = 0$ to t), m is the mass of the polymer, V is the volume of the enclosed room, as well as the concentration of AA in the atmosphere initially and at time t, C_0 and C_{out}, respectively

$$m(Q_{in} - Q_0) = V(C_0 - C_{out}) \quad (9)$$

$$\Rightarrow Q_{in} = \frac{VC_0 + mQ_0}{m + \frac{V}{K'_H}} \quad (10)$$

Comparison with Experimental Data. After considering the kinetics and mass balance, a set of equations (eq 2 for acid-catalyzed and noncatalyzed degradation channels and eq 10 for mass balance) can be used to predict the long-term deacetylation of CA. In the current work, calculations with the transition-state theory, to obtain the reaction constant, are made by considering a pseudo-one-step reaction with the energy barrier given from the highest value observed in the reaction mechanism. An alternative way would be to use the values of the standard molar Gibbs energies (Table 1). However, in the latter, the concentration of the intermediate should be considered when taken as the reference state in the second step of the reaction. The water concentration, eq 5, and the AA concentration, eq 10, were implemented in eq 2. The ordinary differential equation (eq 2) was solved, as a function of time, using the ODE solver, ode23, provided in the software package MATLAB/SIMULINK. The evolution of the concentrations of water and AA was accounted for at each instant by the solver. It is important to note that these equations are all introduced to the MATLAB ODE solver and solved as a function of time, simultaneously. The two degradation pathways are considered bimolecular (water and acetate group are involved; protonation of the acetate group is

https://dx.doi.org/10.1021/acsomega.0c05438
ACS Omega 2021, 6, 8028−8037

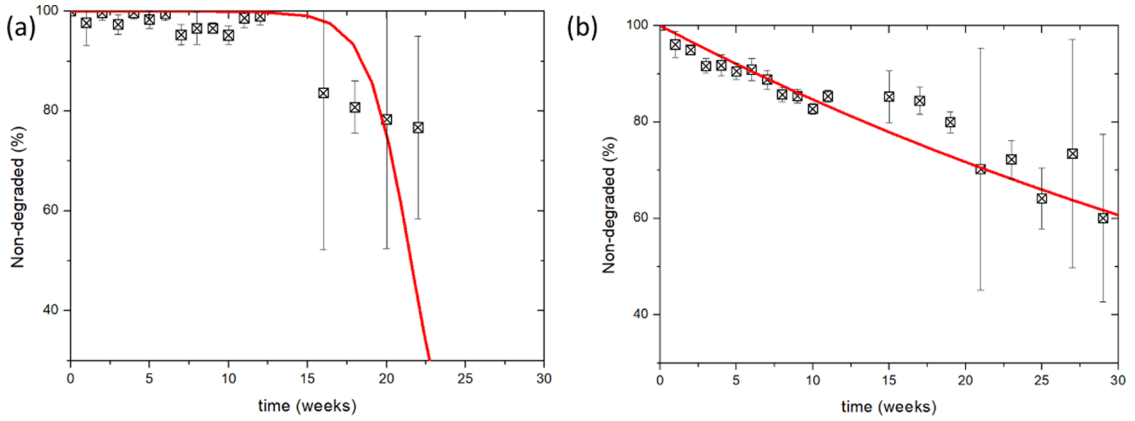

Figure 3. Experimental degradation profiles of the CDA polymer. Experimental data is shown in squares along with the corresponding standard deviation for each point, while the model prediction is represented by the solid red line for the (a) thermal aging conditions at 80 °C and RH = 100%, and (b) acidic aging conditions at 70 °C, RH = 80%, and constant AA concentration of 1.7899×10^{-5} mmol/cm^3 in the gas phase.

very quick) and solved simultaneously. However, to be applied to a particular situation, several parameters need to be defined and adjusted to that case. Below, this application is demonstrated for the experimental conditions used for accelerated aging (forcing temperature and constant acidic conditions). This is useful to understand how the model can be applied and also to validate the model upon comparing the experimental results with the simulated ones.

During the thermal aging experiments, samples of ca. 1.2 g were placed in a closed chamber with a total free volume (V) of 11 588 cm^3. In this chamber, the initial concentration of AA is zero (initial boundary condition). Henry's constant for these conditions (K'_H) was estimated using eq 8 considering 80 °C, with an average value of K_H = 21.2 mmol/g and the values of p^0 taken from the Dortmund Data Bank.[33] Substituting these values into eq 10, we obtain a relation of $Q_{in} = 0.139Q_o$ for these conditions.

For the acidic aging set of experiments, the total mass of the CDA films was also ca. 1.2 g, placed in a chamber with a volume of 2550 cm^3 at 70 °C. The initial concentration of AA, which corresponds to the AA vapor phase concentration, was maintained as constant as possible throughout the experiment at 1.7899×10^{-5} mmol/cm^3 (see the Computational Methods). Thus, for these conditions, the concentration of AA inside the polymer is rather dictated by the constant AA concentration imposed by the aqueous solution in the atmosphere. Thus, from eq 7, we get Q_{in} = 0.0582 mmol/g.

Another important detail is the pH of the medium, which will be altered by the concentration of AA produced. Considering the AA dissociation constant[34] $K_a = 1.8 \times 10^{-5}$, the pH can be calculated as $\mathrm{pH} = -\log(\sqrt{Q_{AA}K_a})$, with Q_{AA} being the concentration of AA inside the film in mol/L at any particular time. The dissociation constant of AA in water was used in this case, although we recognize that the constant for the reaction of AA with water inside the polymer may be different. However, the determination of the dissociation constant inside the polymer is not straightforward, and since a significant amount of water is present inside the polymer, we assumed it to be the same as in water.

The diffusion of AA in the polymer could be a limiting factor in the degradation process if it is very slow compared with the reaction kinetics, *i.e.*, the reaction would be limited by the diffusion. In that case, the kinetics of diffusion should have been considered along with the reaction kinetics. However, for AA inside the CA polymer, the diffusion coefficient (D) was reported to be 1.2×10^{-14} m^2/s at 25 °C.[35] Applying the diffusion law, for a typical CA film (thickness of around 200 μm), the time required to cross half of the film, taking into account that AA can escape from both sides, is around 10 days. This diffusion process is quite slow (many days); however, the degradation process at a temperature of 25 °C is found to take hundreds of years (see below). At the temperature conditions used in the experiments (above room temperature), the diffusion time will be even shorter. For this reason, we can assume that the influence of the diffusion kinetics is much quicker than that of degradation. In other words, we can consider that the diffusion of AA inside CA is not the limiting step and its effect on the kinetic model can be neglected.

Finally, the model can be applied to estimate the degradation of CDA samples over time, and the results are compared with the artificial aging experimental results. To help with the comparison, the experimental degree of degradation was determined considering the DS. The initial DS of the pure laboratory-grade polymer used is 2.46; this DS corresponds to 100% non-degraded. The results from the model reported the variation of concentrations of acetyl groups in CDA in mmol/g, and this was also transformed to percentage of degradation upon considering the initial concentration C_0 as 100% nondegraded. Figure 3a shows the experimental data obtained with the thermal conditions along with the model results considering the same conditions. A good agreement was obtained for the early stages of degradation, indicating the ability of the model to predict the onset of the degradation of the CDA polymer. As can be observed, the model predicts very well the critical point where the polymer degradation starts to accelerate with a significant decrease in the acetylation degree in just a few days. Note that this critical point is very important from the perspective of the conservation of the objects and artifacts made of CDA, because from that point forward, the degradation rate is substantially accelerated and the objects or artworks will be lost very quickly. It is important to highlight that the practical interest of this model lies in the slightly degraded region, where the accuracy of the measurements is better as well as the initial assumptions for the model. After the critical point, an increased standard deviation error is observed, making it difficult to confirm the quality of the fit at advanced stages of degradation. This is attributed to the nonhomogeneous nature of the polymer's degradation process, as can be

https://dx.doi.org/10.1021/acsomega.0c05438
ACS Omega 2021, 6, 8028−8037

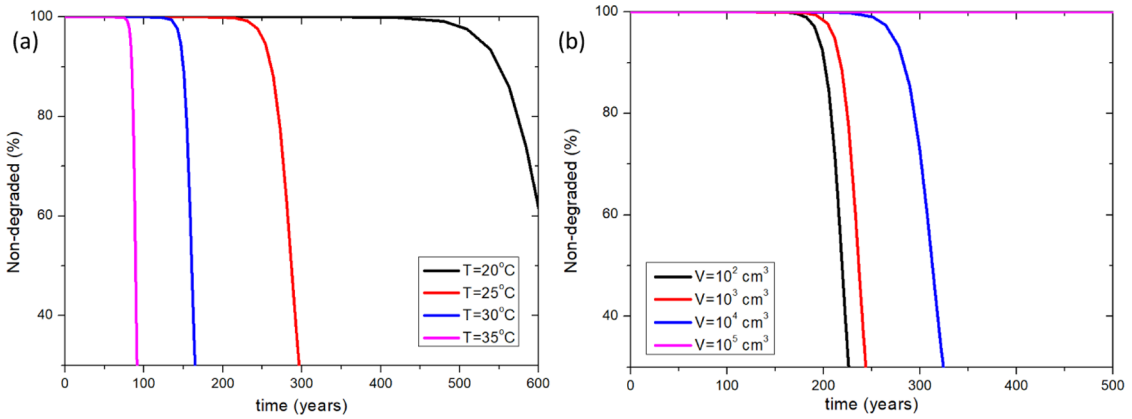

Figure 4. Estimation of the effect of temperature and volume storage conditions close to real-condition scenarios. (a) Temperature effect on a 1 g polymer inside a 100 cm^3 free volume chamber and (b) volume effect on a 1 g polymer at a constant temperature of 27 °C with RH = 40%.

observed in Figure S3. After 15 weeks of aging for both tests, thermal and acid-catalyzed, some regions inevitably degraded faster than others due to the autocatalytic effect of the acetic acid formation. An average of three μFTIR spectra was taken over these different-degradation-state regions. This protocol increases the standard deviation error but gives a more correct image of the degradation process. After week 22, the obtained experimental data (not presented) did not make sense: the degree of substitution was increasing. This situation can probably be explained by a change in the mechanism, due to the simultaneous occurrence of chain scission in the ether bond between the anhydroglucose rings. As the C−O−C bond was considered the unchanged FTIR reference peak for DS determination, it means that the calibration curve was not valid anymore (also our mechanistic model only takes into account the deacetylation contribution). Nevertheless, at these high degradation stages, the objects made of CDA would be almost lost and the prediction of degradation would not be very useful anymore.

The results for the acidic aging condition (Figure 3b) show a fast start of degradation since the first weeks of the experiment due to the presence of AA concentration in the atmosphere, which can enter the polymer and catalyze the degradation. This phenomenon is quite relevant when contamination of historical films in good preservation condition occurs. A kickoff of their degradation is given, which if not detected on time can result in a total loss of a collection. This quantitative study aims precisely to avoid the occurrence of such situations. The results also show that the attempt of keeping the concentration constant influences the concentration of AA inside the polymer and stabilizes the rate of degradation at later stages. In other words, the solubility of AA in the aqueous solution present in the acidic conditions experiments acted as a sink. Thus, at later degradation stages, the degradation rate in thermal artificial aging is higher than in the acidic conditions due to the AA accumulation. As shown in the graphic, for the equivalent period of time needed for the critical point of the noncatalyzed degradation (13−15 weeks), the catalytic reaction begins to have a nonhomogeneous behavior, shown by the increase of the measurements' error bar; the enhancement of the DS standard deviation might probably be due to a smaller extent of chain scission reaction starting to occur. This set of experiments emphasizes the importance of AA accumulation in the atmosphere on the degradation kinetics and sheds some light on the complexity of the DCA degradation pathway. Again, the comparison of the degradation predicted using the model is in very good agreement with the experimental data (Figure 3b).

Predicting Real-Life Scenarios. The main goal of having this type of model to predict polymer degradation is to be able to anticipate the long-term behavior of the polymers under different storage/use conditions. This information may give indications on the best strategies and conditions regarding the preservation of objects made from that polymer. To this aim, several possible conditions were applied to the model to analyze the differences in the predicted behavior of the CDA polymer. For example, considering 1 g of CDA polymer inside a free closed volume of 100 cm^3, the results (Figure 4a) show a strong effect of temperature change in the lifetime of the polymer. As the temperature increases slightly (15 °C between the lowest and highest temperatures considered), a significant impact on the degradation kinetics is observed because the time to reach 70% goes from 100 to 450 years when changing the temperature from 35 to 25 °C. It is worth mentioning that in real conditions, at very advanced degradation stages, the diffusion process may become a limiting step of the reaction rate, thus leading to a softening in the steep decrease. However, the practical interest of the developed model lies in the slightly degraded regions to predict when the degradation starts to accelerate significantly, to decide on preventive actions to take before a total loss of the material. It is important to point out that other parameters, like Henry's constant, are only valid at low acetic acid concentrations and low degradation stages, which are the regions of interest in our work. In Figure 4b, the effect of volume that encompasses the polymer is shown, maintaining the mass and temperature constant. We notice that large volumes slow down the degradation rates, *i.e.*, considering as reference 70% of the nondegraded fraction, the time to reach this value increases from 350 to 450 years when increasing the volume from 100 to 10 000 cm^3. This effect is due to the lowering of the accumulation of AA in the surrounding atmosphere when the volume increases. This forces the concentration inside the polymer to be lower, thus slowing down the rate of the deacetylation reaction. However, having a sufficiently large chamber introduces practical storage problems of space resources and dust accumulation. The bigger volumes could actually be replaced by an effective adsorbent that clears the atmosphere of the released AA,[36] but other critical aspects should also be considered to define a practical conservation strategy. Contrary to volume and

https://dx.doi.org/10.1021/acsomega.0c05438
ACS Omega 2021, 6, 8028−8037

temperature, RH did not prove to be a critical parameter in this study.

We consider this new model useful for the conservation field. Several studies have been performed to address this issue, but they were mainly data-based models that are applicable only to that particular situation, also without a deep understanding of the underlying processes. For example, most of this information in the field of photography is shown as a plot of acidity versus time without a quantitative scale for the axis system.[8,11] The model provided in this work may contribute to a better understanding and prediction of the degradation processes in complex systems where CDA is present.

CONCLUSIONS

We presented a new methodology to estimate the long-term stability of a widely used semisynthetic polymer: cellulose diacetate. The approach successfully couples DFT calculations with the TST theory to estimate the deacetylation reaction rates of the CDA polymer. Insights into the mechanisms of acid-catalyzed and noncatalyzed reactions obtained by DFT calculations of the transition state demonstrated that the presence of the proton (acid-catalyzed) decreases significantly the activation energy of the first step of the reaction (about 20 kcal/mol), compared with the noncatalyzed path. This reduction justifies the faster rate of the acid-catalyzed reaction path. To complete the model, the concentration of AA—the reaction product—inside the polymer was experimentally determined for the first time as a function of the partial pressure on the surrounding atmosphere, *i.e.*, Henry's constant for the phase equilibria. This allowed one to determine the concentration of reactants inside the polymer with time.

The application of the developed model was demonstrated and validated by comparing it with experimental results of accelerated aging. A good agreement was observed without any adjustable parameter giving an accurate description of the autocatalytic dominant behavior, *i.e.*, the acceleration of the degradation rate. The model provides answers about the fundamental behavior of the polymer and the role of AA in accelerating the degradation process, accounting for the dependence of the degradation process on the following parameters: temperature, relative humidity, and pH. The model gives quantitative predictions on the amount of AA being released depending on the mass of the polymer stored in a specific volume and the influence of the surrounding environment's AA concentration on the reaction rate. It also helps in understanding how the acidity of the surrounding environment influences the degradation of CDA. This is known to occur in the conservation field, when there is cross-contamination from an object at an advanced degradation stage to other objects in the vicinity.

We consider this model as a fundamental building block toward understanding/predicting the behavior of CA in all CA-polymer-integrated applications of real polymer blends and composites that are more complex. Also, the strategy presented in this work may be extrapolated to other types of polymers and associated degradation mechanisms since we opted for general first-principles-based modeling.

ASSOCIATED CONTENT

Supporting Information

The Supporting Information is available free of charge at https://pubs.acs.org/doi/10.1021/acsomega.0c05438.

Experimental results and the justification of the linear dependence of the concentration of AA on the CDA polymer with the partial pressure of AA to determine Henry's constant; determination of the dependence of K_H on temperature and aging of the polymer; details on the data fitting of the dependence of water concentration on temperature, relative humidity, and pH (PDF)

Video showing the imaginary frequencies of the transition states of both reaction steps for deacetylation under neutral and acid-catalyzed conditions (MP4)

AUTHOR INFORMATION

Corresponding Authors

Abeer Al Mohtar − *CERENA, Departamento de Engenharia Química, Instituto Superior Técnico, Universidade de Lisboa, 1049-001 Lisboa, Portugal;* orcid.org/0000-0002-9212-1269; Email: abeer.mohtar@tecnico.ulisboa.pt

Moisés L. Pinto − *CERENA, Departamento de Engenharia Química, Instituto Superior Técnico, Universidade de Lisboa, 1049-001 Lisboa, Portugal;* orcid.org/0000-0003-3061-9632; Email: moises.pinto@tecnico.ulisboa.pt

Authors

Sofia Nunes − *LAQV−REQUIMTE, Departamento de Química, Faculdade de Ciências e Tecnologia, Universidade NOVA de Lisboa, 2829516 Monte De Caparica, Portugal*

Joana Silva − *LAQV−REQUIMTE, Departamento de Química, Faculdade de Ciências e Tecnologia, Universidade NOVA de Lisboa, 2829516 Monte De Caparica, Portugal*

Ana Maria Ramos − *LAQV−REQUIMTE, Departamento de Química, Faculdade de Ciências e Tecnologia, Universidade NOVA de Lisboa, 2829516 Monte De Caparica, Portugal*

João Lopes − *iMED.Ulisboa, Faculdade de Farmácia, Universidade de Lisboa, 1649-003 Lisboa, Portugal*

Complete contact information is available at: https://pubs.acs.org/10.1021/acsomega.0c05438

Notes

The authors declare no competing financial interest.

ACKNOWLEDGMENTS

This work has received funding from the European Union's Horizon 2020 research and innovation program under grant agreement no. 760801\NEMOSINE. Fundação para a Ciência e a Tecnologia (FCT-MCTES) is acknowledged for the funding to the Projects UIDB/04028/2020 and UIDP/04028/2020 (CERENA) and to the Project UID/QUI/50006/2019 (Associated Laboratory for Sustainable Chemistry−Clean Processes and Technologies, LAQV−REQUIMTE).

REFERENCES

(1) Lendlein, A.; Langer, R. Biodegradable, Elastic Shape-Memory Polymers for Potential Biomedical Applications. *Science* **2002**, *296*, 1673−1676.

(2) Stuart, M. A. C.; Huck, W. T. S.; Genzer, J.; Müller, M.; Ober, C.; Stamm, M.; Sukhorukov, G. B.; Szleifer, I.; Tsukruk, V. V.; Urban, M.; Winnik, F.; Zauscher, S.; Luzinov, I.; Minko, S. Emerging Applications of Stimuli-Responsive Polymer Materials. *Nat. Mater.* **2010**, *9*, 101−113.

(3) Li, G.; Zhu, R.; Yang, Y. Polymer Solar Cells. *Nat. Photonics* **2012**, *6*, 153−161.

(4) Borup, R.; Meyers, J.; Pivovar, B.; Kim, Y. S.; Mukundan, R.; Garland, N.; Myers, D.; Wilson, M.; Garzon, F.; Wood, D.; Zelenay,

P.; More, K.; Stroh, K.; Zawodzinski, T.; Boncella, J.; McGrath, J. E.; Inaba, M.; Miyatake, K.; Hori, M.; Ota, K.; Ogumi, Z.; Miyata, S.; Nishikata, A.; Siroma, Z.; Uchimoto, Y.; Yasuda, K.; Kimijima, K. I.; Iwashita, N. Scientific Aspects of Polymer Electrolyte Fuel Cell Durability and Degradation. *Chem. Rev.* **2007**, 3904−3951.
(5) Jørgensen, M.; Norrman, K.; Krebs, F. C. Stability/Degradation of Polymer Solar Cells. *Sol. Energy Mater. Sol. Cells* **2008**, *92*, 686−714.
(6) Allen, N. S.; Edge, M. *Polymer Degradation and Stabilisation*; Springer, 1986; Vol. *7*.
(7) Schnabel, W. *Polymer Degradation, Principles and Practical Applications*; Carl Hanser Verlag: Munich, 1981; Vol. *87*.
(8) Lavédrine, B. *A Guide to the Preventive Conservation of Photograph Collections*; Getty Publications: Los Angeles, 2003.
(9) Littlejohn, D.; Pethrick, R. A.; Quye, A.; Ballany, J. M. Investigation of the Degradation of Cellulose Acetate Museum Artefacts. *Polym. Degrad. Stab.* **2013**, *98*, 416−424.
(10) McGath, M.; Jordan-Mowery, S.; Pollei, M.; Heslip, S.; Baty, J. Cellulose Acetate Lamination: A Literature Review and Survey of Paper-Based Collections in the United States. *Restaurator* **2015**, *36*, 333−365.
(11) Krause, P.; Kraus, P.; Reilly, J. P.; Reilly, J. M. IPI Storage Guide for Acetate Film. *J. Am. Inst. Conserv.* **1994**, *33*, 321.
(12) Reilly, J. M.; Nishimura, D. W.; Zinn, E. *New Tools for Preservation Assessing Long-Term Environmental Effects on Library and Archives Collections*; Commission on Preservation and Access, 1995.
(13) Michalski, S. In *Double the Life for Each Five-Degree Drop, More than Double the Life for Each Halving of Relative Humidity*, ICOM Committee for Conservation, 13th Triennial Meeting, Rio de Janeiro, Sept 22−27, 2002; pp 66−72.
(14) Ahmad, I. R.; Cane, D.; Townsend, J. H.; Triana, C.; Mazzei, L.; Curran, K. Are We Overestimating the Permanence of Cellulose Triacetate Cinematographic Films? A Mathematical Model for the Vinegar Syndrome. *Polym. Degrad. Stab.* **2020**, *172*, No. 109050.
(15) Labanowski, J. K.; Andzelm, J. W. *Density Functional Methods in Chemistry*; Springer Science & Business Media, 1991.
(16) Frisch, M. J.; Trucks, G. W.; Schlegel, H. B.; Scuseria, G. E.; Robb, M. A.; Cheeseman, J. R.; Scalmani, G.; Barone, V.; Mennucci, B.; Petersson, G. A.; Nakatsuji, H.; Caricato, M.; Li, X.; Hratchian, H. P.; Izmaylov, A. F.; Bloino, J.; Zheng, G.; Sonnenberg, J. L.; Hada, M.; Ehara, M.; Toyota, K.; Fukuda, R.; Hasegawa, J.; Ishida, M.; Nakajima, T.; Honda, Y.; Kitao, O.; Nakai, H.; Vreven, T.; Montgomery, J. A.; Peralta, J. E.; Ogliaro, F.; Bearpark, M.; Heyd, J. J.; Brothers, E.; Kudin, K. N.; Staroverov, V. N.; Kobayashi, R.; Normand, J.; Raghavachari, K.; Rendell, A.; Burant, J. C.; Iyengar, S. S.; Tomasi, J.; Cossi, M.; Rega, N.; Millam, J. M.; Klene, M.; Knox, J. E.; Cross, J. B.; Bakken, V.; Adamo, C.; Jaramillo, J.; Gomperts, R.; Stratmann, R. E.; Yazyev, O.; Austin, A. J.; Cammi, R.; Pomelli, C.; Ochterski, J. W.; Martin, R. L.; Morokuma, K.; Zakrzewski, V. G.; Voth, G. A.; Salvador, P.; Dannenberg, J. J.; Dapprich, S.; Daniels, A. D.; Farkas; Foresman, J. B.; Ortiz, J. V.; Cioslowski, J.; Fox, D. J.. *Gaussian 09*, revision B.01; Gaussian, Inc.: Wallingford, CT, 2009.
(17) Becke, A. D. Density-Functional Thermochemistry. III. The Role of Exact Exchange. *J. Chem. Phys.* **1993**, *98*, 5648−5652.
(18) Xia, S.; Zhang, H. Density Functional Theory Study of Selective Deacylation of Aromatic Acetate in the Presence of Aliphatic Acetate under Ammonium Acetate Mediated Conditions. *J. Org. Chem.* **2014**, *79*, 6135−6142.
(19) Espenson, J. H. *Chemical Kinetics and Reaction Mechanisum*, 2nd ed.; McGraw-Hill, Inc.: New York, 1995; Vol. *102*.
(20) Cruz, A. J.; Pires, J.; Carvalho, A. P.; Brotas de Carvalho, M. Comparison of Adsorbent Materials for Acetic Acid Removal in Showcases. *J. Cult. Heritage* **2008**, *9*, 244−252.
(21) Hayden, J. G.; O'Connell, J. P. A Generalized Method for Predicting Second Virial Coefficients. *Ind. Eng. Chem. Process Des. Dev.* **1975**, *14*, 209−216.
(22) Hsieh, C. T.; Lee, M. J.; Lin, H. M. Multiphase Equilibria for Mixtures Containing Acetic Acid, Water, Propylene Glycol Monomethyl Ether, and Propylene Glycol Methyl Ether Acetate. *Ind. Eng. Chem. Res.* **2006**, *45*, 2123−2130.
(23) Zhang, M.; Chen, L.; Yang, H.; Ma, J. Vapor Liquid Equilibria for Acetic Acid-Acetaldehyde-Crotonaldehyde System: Gibbs Ensemble Molecular Simulation for Pure Components and Binary Systems and NRTL Model Prediction for Ternary System. *Ind. Eng. Chem. Res.* **2018**, *57*, 2353−2364.
(24) Cruz, A. J.; Pires, J.; Carvalho, A. P.; De Carvalho, M. B. Adsorption of Acetic Acid by Activated Carbons, Zeolites, and Other Adsorbent Materials Related with the Preventive Conservation of Lead Objects in Museum Showcases. *J. Chem. Eng. Data* **2004**, *49*, 725−731.
(25) MacDougall, F. H. The Molecular State of the Vapor of Acetic Acid at Low Pressures at 25, 30, 35 and 40°. *J. Am. Chem. Soc.* **1936**, *58*, 2585−2591.
(26) Fei, P.; Liao, L.; Cheng, B.; Song, J. Quantitative Analysis of Cellulose Acetate with a High Degree of Substitution by FTIR and Its Application. *Anal. Methods* **2017**, *9*, 6194−6201.
(27) Nunes, S.; Ramacciotti, F.; Neves, A.; Angelin, E. M.; Ramos, A. M.; Roldão, É.; Wallaszkovits, N.; Armijo, A. A.; Melo, M. J. A Diagnostic Tool for Assessing the Conservation Condition of Cellulose Nitrate and Acetate in Heritage Collections: Quantifying the Degree of Substitution by Infrared Spectroscopy. *Heritage Sci.* **2020**, *8*, No. 33.
(28) Samios, E.; Dart, R. K.; Dawkins, J. V. Preparation, Characterization and Biodegradation Studies on Cellulose Acetates with Varying Degrees of Substitution. *Polymer* **1997**, *38*, 3045−3054.
(29) Adelstein, P. Z.; Bigourdan, J.-L.; Reilly, J. M. Moisture Relationships of Photographic Film. *J. Am. Inst. Conserv.* **1997**, *36*, 193.
(30) Allen, N. S.; Edge, M.; Rorie, C. V.; Jewitt, T. S.; Appleyard, J. H. The Degradation and Stabilization of Historic Cellulose Acetate/Nitrate Base Motion-Picture Film. *J. Photogr. Sci.* **1988**, *36*, 103−106.
(31) Lavédrine, B.; Borenstein, D.; Dubail, M.; Furdygiel, B.; Garnier, C.; Gillet, M.; Langlois, G.; Nguyen, T.-P.; Malalanirina, S. *Biocontamination at the French Film Archives: Study of Its Origin and Its Remediation*; Indiana University Press, 2017.
(32) Pinto, M. L.; Pires, J.; Carvalho, A. P.; De Carvalho, M. B.; Bordado, J. C. Sorption Isotherms of Organic Vapors on Polyurethane Foams. *J. Phys. Chem. B* **2004**, *108*, 13813−13820.
(33) Dortmund Data Bank. www.ddbst.com.
(34) Hieble, J. P. Animal Models for Benign Prostatic Hyperplasia. In *Urinary Tract*; Andersson, K. E.; Michel, M., Eds.; Handbook of Experimental Pharmacology; Springer, 2011; Vol. *2011*, pp 69−79.
(35) Zhang, X. R.; Zhang, L. Z.; Pei, L. X. Sorption, Permeation and Selective Transport of Moisture/VOCs through a CA Membrane for Total Heat Recovery. *Int. J. Low-Carbon Technol.* **2013**, *8*, 64−69.
(36) Dedecker, K.; Pillai, R. S.; Nouar, F.; Pires, J.; Steunou, N.; Dumas, E.; Maurin, G.; Serre, C.; Pinto, M. L. Metal-Organic Frameworks for Cultural Heritage Preservation: The Case of Acetic Acid Removal. *ACS Appl. Mater. Interfaces* **2018**, *10*, 13886−13894.

https://dx.doi.org/10.1021/acsomega.0c05438
ACS Omega 2021, 6, 8028−8037